Dispersion Analysis of Multilayer Cylindrical Transmission Lines Containing Magnetized Ferrite Substrates

Nihad Dib, *Senior Member, IEEE,* and Amjad Omar

***Abstract*—Recently, there has been a growing interest in using cylindrical transmission lines that contain magnetized ferrite material in a variety of applications. In this paper, the finite-difference time-domain (FDTD) method (in cylindrical coordinates) and the spectral-domain analysis (SDA) are used to calculate the propagation characteristics of cylindrical transmission lines that contain magnetized ferrite material. The magnetization can be either in the longitudinal or azimuthal directions. Specifically, the cylindrical microstrip line, and the cylindrical coplanar waveguide printed on magnetized ferrite substrate are analyzed. Both the FDTD and SDA results are in very good agreement. In addition, the results are compared to those of planar structures by taking the radius of the substrate to be large enough such that the curvature effect is negligible.**

***Index Terms*—Circular waveguide, coplanar waveguide, FDTD methods, ferrite loaded waveguides, microstrip, spectral-domain analysis.**

I. Introduction

THERE IS A growing interest in antennas that are printed on cylindrical substrates. These antennas may find applications in aircraft, missiles, and wireless communications due to their features of conformability, light weight, small size, and the geometrical compatibility to the vehicle they are mounted on. The use of ferrite substrates also adds more flexibility to the design of cylindrical antennas due to the effect of the applied dc magnetic field on the performance of the antenna.

Ferrite materials are widely used in microwave applications, such as isolators, circulators, and phase shifters. Recently, there has been an increasing interest in studying cylindrical structures (circular waveguide and cylindrical microstrip antennas) containing magnetized ferrite media [1]–[6]. Specifically, the effects of anisotropy of ferrite coating on the radiation characteristics of cylindrical structures excited by elementary electric or magnetic dipoles have been investigated in [1]–[3]. The main advantage of a ferrite substrate is that the electrical parameters can be controlled by an externally applied magnetic field.

Recently, the finite-difference time-domain (FDTD) technique has been extended to study the dispersion characteristics of cylindrical transmission lines containing isotropic multilayered dielectrics [7], [10]. In this paper, the FDTD technique, in cylindrical coordinates, is extended to study the dispersion characteristics of cylindrical lines that might contain magnetized ferrite media. The magnetization could be in the longitudinal or azimuthal directions. The extension of the rectangular FDTD to the analysis of structures with ferrite material has been the subject of many papers in the literature [11]–[22]. In this paper, the extension of the cylindrical FDTD parallels the extended rectangular FDTD algorithm proposed in [11].

Moreover, based on the spectral-domain technique, a simple and general method for solving general two-dimensional (2-D) cylindrical transmission lines that are composed of a mixture of iso/anisotropic substrates is presented. The spectral-domain method is used to analyze cylindrical transmission lines with longitudinally magnetized ferrite substrates and the results are compared to those obtained using the FDTD technique.

Specifically, both the cylindrical microstrip line, and the cylindrical coplanar waveguide (CCPW) with ferrite substrate are analyzed. To our knowledge, such cylindrical lines on magnetized ferrite substrate have not been studied before in the literature. Several examples are included and the numerical results are compared to those of planar structures.

II. Theoretical Formulation

A. FDTD Method

The structure under consideration is a multilayered cylindrical transmission line which may include ferrite media. The ferrite media could be axially or azimuthally magnetized by an external magnetic field. It is assumed that the ferrite is lossless and is in the saturation magnetization status. One starts by discretizing Maxwell's equations in cylindrical coordinates

$$\overline{\nabla} \times \overline{E} = -\frac{\partial \overline{B}}{\partial t} \tag{1}$$

$$\overline{\nabla} \times \overline{H} = \frac{\partial \overline{D}}{\partial t}. \tag{2}$$

Assuming $e^{-j\beta z}$ propagating wave reduces the three–dimensional (3-D) finite-difference mesh to an equivalent 2-D one [7]. Fig. 1 shows the equivalent 2-D cell obtained by compressing the 3-D cell in the z direction. The components of the magnetic flux density $\overline{B}$ are at the same positions of those of the magnetic

Manuscript received March 25, 2001.

N. Dib is with the Ansoft Corporation, Elmwood Park, NJ 07407 USA, on leave from the Electrical Engineering Department, Jordan University of Science and Technology, Irbid, Jordan.

A. Omar is with the Department of Electrical and Computer Engineering, Hashemite University, Zarqa, Jordan.

Publisher Item Identifier 10.1109/TMTT.2002.800423.

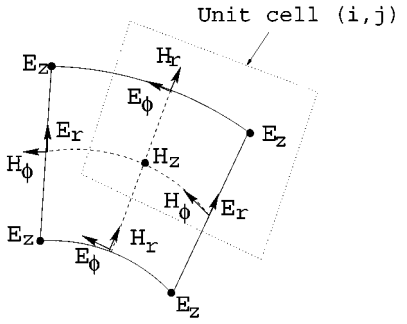

Fig. 1. Typical 2-D FDTD cell in cylindrical coordinate system.

field intensity $\overline{H}$. Discretizing (1) according to the 2-D cell gives the following three difference equations for B_r, B_ϕ, and B_z:

$$\begin{aligned} &B_r^{n+(1/2)}(i,j) \\ &\quad = B_r^{n-(1/2)}(i,j) - j\beta\triangle t E_\phi^n(i,j) \\ &\qquad + \triangle t\left[\frac{E_z^n(i,j-1) - E_z^n(i,j)}{i\triangle\phi\triangle r}\right] \end{aligned} \tag{3}$$

$$\begin{aligned} &B_\phi^{n+(1/2)}(i,j) \\ &\quad = B_\phi^{n-(1/2)}(i,j) + j\beta\triangle t E_r^n(i,j) \\ &\qquad + \triangle t\left[\frac{E_z^n(i,j) - E_z^n(i-1,j)}{\triangle r}\right] \end{aligned} \tag{4}$$

$$\begin{aligned} &B_z^{n+(1/2)}(i,j) \\ &\quad = B_z^{n-(1/2)}(i,j) \\ &+ \triangle t\left\{\left[\frac{E_r^n(i,j) - E_r^n(i,j-1)}{(i-0.5)\triangle r\triangle\phi}\right]\right. \\ &\qquad \left. + \left[\frac{(i-1)E_\phi^n(i-1,j) - iE_\phi^n(i,j)}{(i-0.5)\triangle r}\right]\right\}. \end{aligned} \tag{5}$$

In the above, i goes from 1 to N_r and j goes from 1 to N_ϕ, where N_r and N_ϕ are the number of cells in the radial r direction and ϕ direction, respectively.

For a ferrite region, the constitutive relation between $\overline{B}$ and $\overline{H}$ can be written as

$$\overline{B} = \mu_0\left(\overline{H} + \overline{M}\right) \tag{6}$$

where $\overline{M}$ is the magnetization vector which is related to $\overline{H}$ through the equation of motion

$$\frac{\partial\overline{M}}{\partial t} = \gamma\mu_0\left(\overline{M}\times\overline{H}\right) \tag{7}$$

where $\gamma = -1.759\times 10^{11}\ \mathrm{s^{-1}T^{-1}}$ is the gyromagnetic ratio.

1) Azimuthal Magnetization: Assuming that the ferrite is biased in the $\hat{\phi}$ direction, and using the small-signal approximation, (7) reduces to

$$\frac{\partial M_r}{\partial t} = \gamma\mu_0(M_0H_z - M_zH_0) \tag{8}$$

$$\frac{\partial M_\phi}{\partial t} = 0 \tag{9}$$

$$\frac{\partial M_z}{\partial t} = \gamma\mu_0(M_rH_0 - M_0H_r) \tag{10}$$

where H_0 is the internal dc bias field and M_0 is the saturation magnetization.

Discretizing the above equations, and using (6) to relate $\overline{M}$ and $\overline{H}$, one obtains three difference equations for H_r, H_ϕ and H_z. For example, (8) is written first as

$$\begin{aligned} M_r^{n+(1/2)}(i,j) = M_r^{n-(1/2)}(i,j) + \gamma\mu_0\triangle t \\ \cdot\left[M_0H_z^n(i,j) - H_0M_z^n(i,j)\right]. \end{aligned} \tag{11}$$

In the above equation, proper time synchronization is maintained as explained in [11]. Thus, extrapolation is used to compute $H_z^n(i,j)$ and $M_z^n(i,j)$ as follows:

$$H_z^n(i,j) = \tfrac{1}{2}\left[3H_z^{n-1/2}(i,j) - H_z^{n-3/2}(i,j)\right] \tag{12}$$

$$M_z^n(i,j) = \tfrac{1}{2}\left[3M_z^{n-1/2}(i,j) - M_z^{n-3/2}(i,j)\right]. \tag{13}$$

Using this approximation and (6), the following relation is obtained for updating H_r:

$$\begin{aligned} &H_r^{n+1/2}(i,j) \\ &= H_r^{n-1/2}(i,j) + \frac{1}{\mu_0}\left[B_r^{n+1/2}(i,j) - B_r^{n-1/2}(i,j)\right] \\ &\quad - \frac{\gamma\mu_0\triangle t}{2}\left\{(M_0+H_0)\left[3H_z^{n-1/2}(i,j) - H_z^{n-3/2}(i,j)\right]\right. \\ &\qquad \left. + \frac{H_0}{\mu_0}\left[B_z^{n-3/2}(i,j) - 3B_z^{n-1/2}(i,j)\right]\right\}. \end{aligned} \tag{14}$$

Similarly, the following equations are obtained for H_z and H_ϕ:

$$\begin{aligned} &H_z^{n+1/2}(i,j) \\ &= H_z^{n-1/2}(i,j) + \frac{1}{\mu_0}\left[B_z^{n+1/2}(i,j) - B_z^{n-1/2}(i,j)\right] \\ &\quad + \frac{\gamma\mu_0\triangle t}{2}\left\{(M_0+H_0)\left[3H_r^{n-1/2}(i,j) - H_r^{n-3/2}(i,j)\right]\right. \\ &\qquad \left. - \frac{H_0}{\mu_0}\left[3B_r^{n-1/2}(i,j) - B_r^{n-3/2}(i,j)\right]\right\} \end{aligned} \tag{15}$$

$$\begin{aligned} &H_\phi^{n+1/2}(i,j) \\ &= H_\phi^{n-1/2}(i,j) + \frac{j\beta\triangle t}{\mu_0}E_r^n(i,j) \\ &\quad + \triangle t\left[\frac{E_z^n(i,j) - E_z^n(i-1,j)}{\mu_0\triangle r}\right]. \end{aligned} \tag{16}$$

It should be noted that setting γ to zero in the above equations reduces to the constitutive relations in a nonmagnetic isotropic medium.

Moreover, to insure space synchronization, interpolation is used to compute H_z and B_z in (14), and B_r and H_r in (15) [11].

Thus, the algorithm proceeds as follows: first, compute $\overline{B}$ from (3)–(5); second, compute $\overline{H}$ from (14)–(16); and finally compute $\overline{E}$ using the difference equations resulting from discretizing (2) [7]. To solve the above difference equations, a value for β has to be selected first as an input parameter. Then, the

peaks in the frequency spectrum are located to determine the eigenvalues of the dominant and higher order modes [7]. One can also consult [7] regarding the stability condition, the absorbing boundary condition used to truncate the mesh in the radial direction, the removal of the singularity at the origin of the mesh ($r = 0$), and the method used to find the characteristic impedance.

2) Longitudinal Magnetization: Assuming that the ferrite is biased in the longitudinal ($\hat{z}$) direction, and using a procedure similar to the above, one obtains the following equations for updating the magnetic field components:

$$\begin{aligned} H_r^{n+1/2}(i,j) &= H_r^{n-1/2}(i,j) + \frac{1}{\mu_0}\Big[B_r^{n+1/2}(i,j) - B_r^{n-1/2}(i,j)\Big] \\ &\quad - \frac{\gamma\mu_0\triangle t}{2}\Bigg\{(M_0+H_0)\Big[H_\phi^{n-3/2}(i,j) - 3H_\phi^{n-1/2}(i,j)\Big] \\ &\qquad + \frac{H_0}{\mu_0}\Big[3B_\phi^{n-1/2}(i,j) - B_\phi^{n-3/2}(i,j)\Big]\Bigg\} \end{aligned} \tag{17}$$

$$\begin{aligned} H_\phi^{n+1/2}(i,j) &= H_\phi^{n-1/2}(i,j) + \frac{1}{\mu_0}\Big[B_\phi^{n+1/2}(i,j) - B_\phi^{n-1/2}(i,j)\Big] \\ &\quad - \frac{\gamma\mu_0\triangle t}{2}\Bigg\{(M_0+H_0)\Big[3H_r^{n-1/2}(i,j) - H_r^{n-3/2}(i,j)\Big] \\ &\qquad - \frac{H_0}{\mu_0}\Big[3B_r^{n-1/2}(i,j) - B_r^{n-3/2}(i,j)\Big]\Bigg\} \end{aligned} \tag{18}$$

$$\begin{aligned} H_z^{n+(1/2)}(i,j) &= H_z^{n-(1/2)}(i,j) \\ &\quad + \frac{\triangle t}{\mu_0}\Bigg\{\left[\frac{E_r^n(i,j) - E_r^n(i,j-1)}{(i-0.5)\triangle r\,\triangle\phi}\right] \\ &\qquad + \left[\frac{(i-1)E_\phi^n(i-1,j) - iE_\phi^n(i,j)}{(i-0.5)\triangle r}\right]\Bigg\}. \end{aligned} \tag{19}$$

To insure space synchronization, interpolation is used to compute H_ϕ and B_ϕ in (17), and B_r and H_r in (18) [11].

B. Spectral-Domain Analysis (SDA): Longitudinal Magnetization

The first step is to derive the fields inside the ferrite substrate that is magnetized by an axial (z directed) dc magnetic field. In this region, the components of $\overline{B}$ and $\overline{H}$ are related by [23]

$$B_r = \mu H_r - j\mu' H_\phi \tag{20}$$

$$B_\phi = j\mu' H_r + \mu H_\phi \tag{21}$$

$$B_z = \mu_0 H_z. \tag{22}$$

Assuming $e^{-j\beta z}$ field variation along the transmission line, and after some lengthy manipulation [23], the following two coupled differential equations are obtained:

$$\nabla_t^2 E_z + aE_z + bH_z = 0 \tag{23}$$

$$\nabla_t^2 H_z + cH_z + dE_z = 0 \tag{24}$$

where $a = k^2 - k'^2\mu'/\mu$, $b = j\beta\omega\mu_0\mu'/\mu$, $c = \mu_0 k^2/\mu$, $d = -j\beta\omega\mu'\epsilon/\mu$, $k'^2 = \omega^2\mu'\epsilon$, and $k^2 = \omega^2\mu\epsilon - \beta^2$.

To decouple the above two equations, the following substitutions are made:

$$E_z = p_1 u_1 + p_2 u_2 \tag{25}$$

$$H_z = q_1 u_1 + q_2 u_2 \tag{26}$$

where p_1, p_2, q_1, and q_2 are unknown constants. This results in the following two decoupled wave equations:

$$\nabla_t^2 u_1 + s_1 u_1 = 0 \tag{27}$$

$$\nabla_t^2 u_2 + s_2 u_2 = 0 \tag{28}$$

where s_1 and s_2 are the roots of the quadratic equation

$$\begin{vmatrix} a-s & b \\ d & c-s \end{vmatrix} = 0 \tag{29}$$

and $p_1 = s_1$, $p_2 = s_2$, $q_1 = ((s_1 - a)s_1)/b$, and $q_2 = ((s_2 - a)s_2)/b$.

The equations in (27) and (28) are then converted to the spectral domain by assuming $e^{jn\phi}$ field dependence, where n is an integer. The resultant field expressions in the spectral domain are expressed in terms of Bessel and Neuman functions and then substituted in (25) and (26) to yield the axial field components E_z and H_z. The transverse field components can be obtained using the expressions in [23].

Applying the boundary conditions results in two sets of equations whose unknowns are the constants in the field expressions. These equations are given by

$$[M_j]\begin{bmatrix} c_0 \\ c_1 \\ \cdot \\ \cdot \\ c_{n-1} \\ c_n \end{bmatrix} = \begin{bmatrix} 0 \\ 0 \\ \cdot \\ \cdot \\ \tilde{J}_z \\ \tilde{J}_\phi \end{bmatrix} \quad [M_E]\begin{bmatrix} c_0 \\ c_1 \\ \cdot \\ \cdot \\ c_{n-1} \\ c_n \end{bmatrix} = \begin{bmatrix} 0 \\ 0 \\ \cdot \\ \cdot \\ \tilde{E}_z \\ \tilde{E}_\phi \end{bmatrix}. \tag{30}$$

Rearranging the above matrix equations gives

$$[M_E][M_j]^{-1}\begin{bmatrix} 0 \\ 0 \\ \cdot \\ \cdot \\ \tilde{J}_z \\ \tilde{J}_\phi \end{bmatrix} = \begin{bmatrix} 0 \\ 0 \\ \cdot \\ \cdot \\ \tilde{E}_z \\ \tilde{E}_\phi \end{bmatrix}. \tag{31}$$

The above equation can be expressed as

$$Z_{11}\tilde{J}_z + Z_{12}\tilde{J}_\phi = \tilde{E}_z \tag{32}$$

$$Z_{21}\tilde{J}_z + Z_{22}\tilde{J}_\phi = \tilde{E}_\phi \tag{33}$$

where Z_{11}, Z_{12}, Z_{21}, and Z_{22} are the impedance Green's functions.

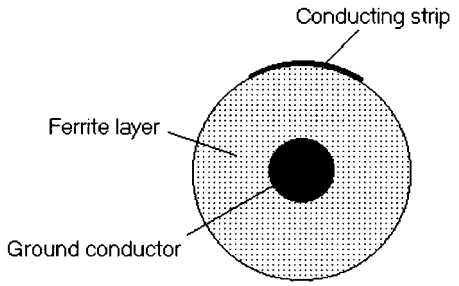

Fig. 2. Cylindrical microstrip line on a ferrite substrate.

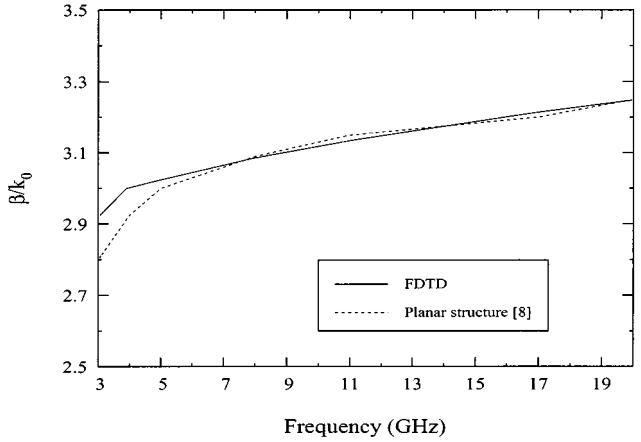

Fig. 3. Phase constant of a cylindrical microstrip line on an azimuthally magnetized ferrite substrate. Ground conductor radius = 3.5 mm, ferrite thickness = 0.5 mm, strip width = 1 mm, $\epsilon_f = 13$, $H_0 = 300$ Oe, and $4\pi M_0 = 1780\ G$.

Expanding the currents $\tilde{J}_z$ and $\tilde{J}_\phi$ in terms of appropriate basis functions that satisfy the edge conditions on the strips results in a matrix equation. The determinant of this equation is equated to zero to find the unknown β.

The above method is versatile in the sense that by simply changing the basis functions for the currents on the strips, other structures such as CPW and CPS can be analyzed.

III. Results and Discussion

In order to test the developed cylindrical 2-D FDTD algorithm, a variety of structures have been investigated and the results were compared with those obtained using other numerical methods. As a first check, the coaxial line and circular waveguide completely filled with longitudinally or azimuthally magnetized ferrite media were analyzed, and the obtained results were within 1% difference from the analytical solutions reported in [4], [5].

A. Cylindrical Microstrip Line

First, a cylindrical microstrip line (Fig. 2), with an azimuthally magnetized ferrite substrate, is considered. The radius of the cylindrical ground of the microstrip line has been taken to be large enough such that the curvature effect on the microstrip characteristics is negligible. This is done to be able to compare our results to those of planar microstrip line printed on a transversely magnetized ferrite substrate. Fig. 3 shows the normalized phase constant (for the forward wave) obtained

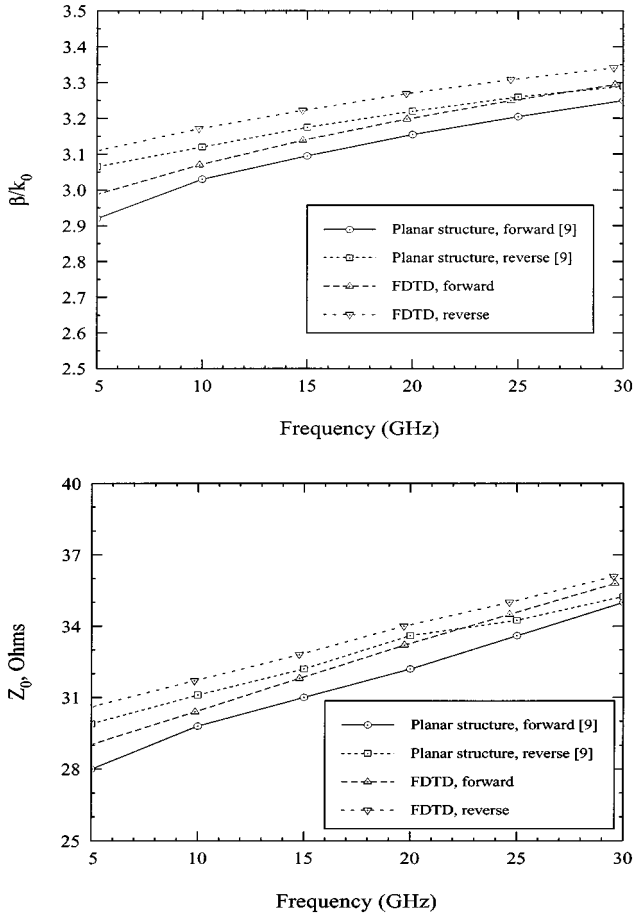

Fig. 4. β/k_0 and Z_0 of a cylindrical microstrip line on a composite dielectric-ferrite substrate. The ferrite is azimuthally magnetized. Ground conductor radius = 2.54 mm, dielectric thickness = 0.254 mm, ferrite thickness = 0.254 mm, strip width = 1.016 mm, $\epsilon_d = 12.9$, $\epsilon_f = 12.6$, $H_0 = 0.1\ M_0$, and $\mu_0 M_0 = 0.275\ T$.

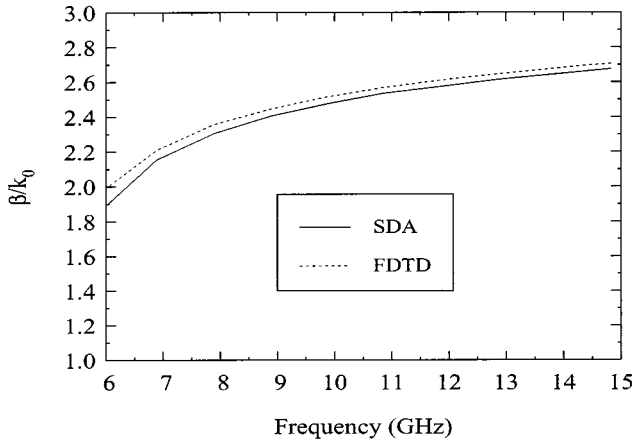

Fig. 5. Phase constant of a cylindrical microstrip line on a longitudinally magnetized ferrite substrate. Ground conductor radius = 3 mm, ferrite thickness = 1 mm, strip width = 1 mm, $\epsilon_f = 10$, $H_0 = 0$, and $4\pi M_0 = 1800\ G$.

using FDTD compared to those reported in [8] for planar microstrip line. It can be seen that the agreement is very good with a maximum difference of 3.5% around 3 GHz, which validates the developed FDTD code for azimuthal magnetization. The difference around 3 GHz could be due to numerical errors in

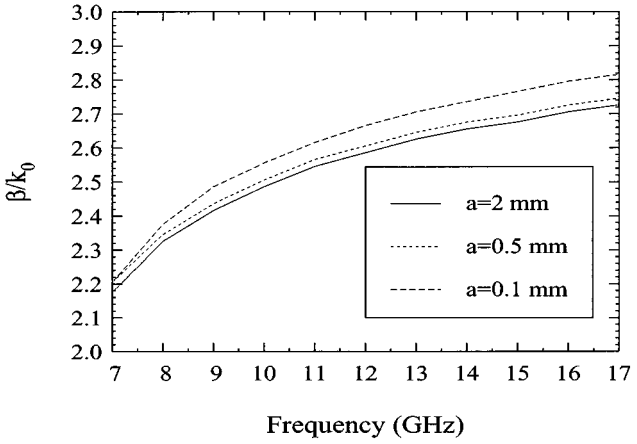

Fig. 6. Effect of the ground conductor radius (a) on the phase constant of a cylindrical microstrip line on a longitudinally magnetized ferrite substrate. SDA results are shown. Ferrite thickness = 1 mm, strip width = 1 mm, $\epsilon_f = 10$, $H_0 = 0$, and $4\pi M_0 = 1800\ G$.

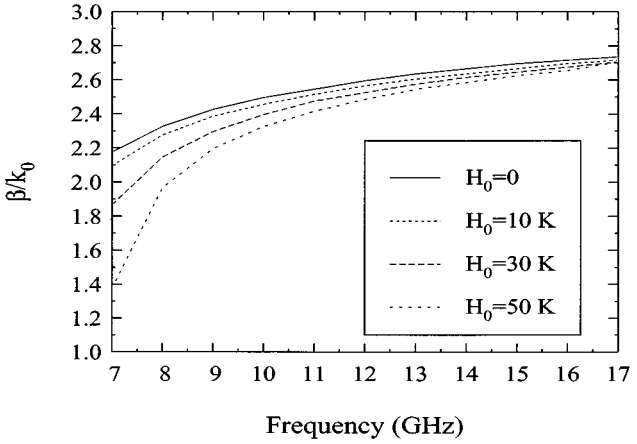

Fig. 7. Effect of H_0 (in A/m) on the phase constant of a cylindrical microstrip line on a longitudinally magnetized ferrite substrate. SDA results are shown. Ground conductor radius = 3 mm, ferrite thickness = 1 mm, strip width = 1 mm, $\epsilon_f = 10$, and $4\pi M_0 = 1800\ G$.

the FDTD analysis and/or the moment method technique used in [8] around the cutoff frequency.

As a second example, Fig. 4 shows the dispersion characteristics (for both forward and reverse waves) of a cylindrical microstrip line printed on a composite dielectric-ferrite substrate. In this structure, a dielectric layer of specific thickness is inserted between the ground and the azimuthally magnetized ferrite layer. Results for the planar structure are taken from [9]. The phase constants obtained using the FDTD are within 2% difference from those reported in [9] for a planar structure. This is due to the fact that the ground conductor radius is relatively large such that the curvature effect is very small. In addition, the characteristic impedance of the same structure obtained using the FDTD is within only 1 Ω from those reported in [9].

Fig. 5 shows the normalized phase constant for a cylindrical microstrip line printed on longitudinally magnetized ferrite obtained using the FDTD and spectral-domain techniques. The agreement is very good between the two methods which validates both of them. Fig. 6 shows the curvature effect on the phase constant by changing the radius of the ground conductor.

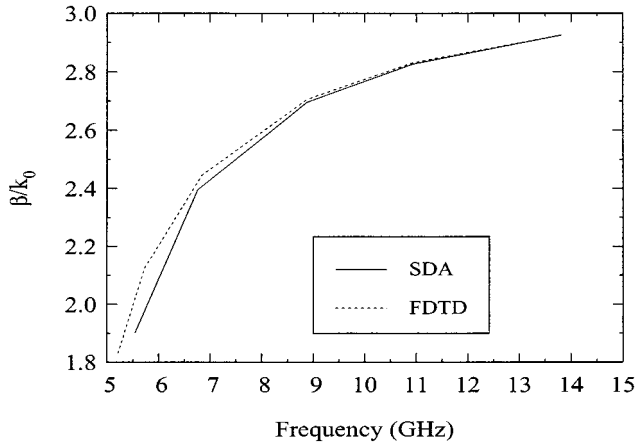

Fig. 8. Normalized phase constant of a cylindrical microstrip line on a longitudinally magnetized ferrite substrate with a dielectric superstrate. Ground conductor radius = 3 mm, ferrite thickness = 1 mm, strip width = 1 mm, dielectric coating thickness = 0.5 mm, $\epsilon_d = 10$, $\epsilon_f = 10$, $H_0 = 0$, and $4\pi M_0 = 1800\ G$.

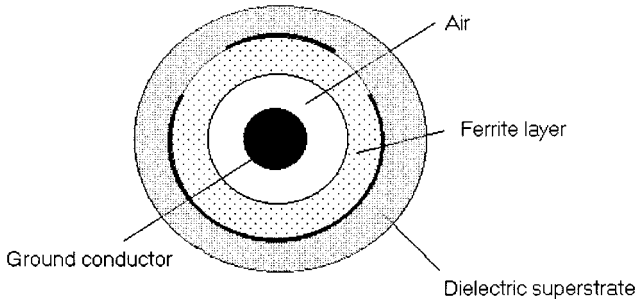

Fig. 9. Multilayered CCPW on a ferrite substrate. Ground conductor radius = 1.9 mm, free-space layer thickness = 0.127 mm, ferrite thickness = 0.5 mm, slot width = center conductor width = 0.25 mm, dielectric superstrate thickness = 0.127 mm, $\epsilon_f = 13$, $\epsilon_d = 2.22$, $H_0 = 1100$ Oe, and $4\pi M_0 = 1780\ G$.

It can be seen that this effect is very small on the phase constant at low frequencies. Fig. 7 shows the effect of the applied bias magnetic field H_0 on the phase constant. It can be seen that the effect of increasing the magnitude of H_0 in the longitudinal direction is more pronounced at lower frequencies, as expected [24].

To show the versatility of the developed FDTD and SD analyses, Fig. 8 shows the normalized phase constant for the structure shown in Fig. 2 with a dielectric coating (superstrate) covering the microstrip line. The dielectric coating has a thickness of 0.5 mm and $\epsilon_d = 10$. The agreement is very good which shows the versatility and validity of the developed analyses.

B. CCPW

Fig. 9 shows a multilayer CCPW structure that is analyzed here. Such a structure is considered so that we can compare our results to those of the shielded planar CPW structure shown in Fig. 10 which has been analyzed in [24] using the finite-element method. Table I shows the results for azimuthal magnetization obtained using the FDTD technique as compared to those presented in [24] for transverse magnetization. The positive phase constant refers to the forward wave, while the negative phase constant refers to the reverse wave since the phase constant exhibits nonreciprocity when H_0 is applied in the azimuthal direc-

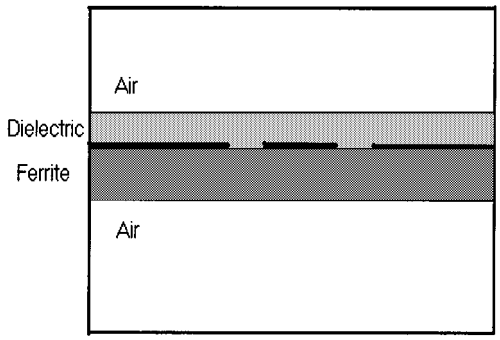

Fig. 10. Multilayered shielded planar CPW on a ferrite substrate with a dielectric superstrate analyzed in [24]. Waveguide width = waveguide height = 3.556 mm, bottom air layer thickness = 0.127 mm, top air layer thickness = 2.8 mm, ferrite thickness = 0.5 mm, slot width = center conductor width = 0.25 mm, dielectric superstrate thickness = 0.127 mm, $\epsilon_f = 13$, $\epsilon_d = 2.22$, $H_0 = 1100$ Oe, and $4\pi M_0 = 1780\ G$.

TABLE I
FDTD RESULTS FOR THE CCPW STRUCTURE SHOWN IN FIG. 9 WITH AZIMUTHAL MAGNETIZATION

β (rad/m)	518	1068	1640	2237	−508	−1047	−1609	−2195
Frequency (FDTD)	9.43	19.22	29.07	38.35	9.05	18.42	28.03	39.02
Frequency [24]	10	20	30	40	10	20	30	40

TABLE II
FDTD RESULTS FOR THE CCPW STRUCTURE SHOWN IN FIG. 9 WITH LONGITUDINAL MAGNETIZATION

β (rad/m)	427	754	1041	1331	1616	1906	2214
Frequency (FDTD)	8.6	13.85	18.74	23.67	28.44	33.22	38.2
Frequency [24]	10	15	20	25	30	35	40

TABLE III
SDA RESULTS FOR THE CCPW STRUCTURE SHOWN IN FIG. 9 WITH LONGITUDINAL MAGNETIZATION

Frequency	10	15	20	25	30	35	40
β/k_0 (SDA)	2.11	2.5	2.6	2.65	2.69	2.72	2.76
β/k_0 [24]	2.04	2.4	2.49	2.54	2.57	2.6	2.64

tion. Tables II and III show the results for longitudinal magnetization for the same structure. In this case, the transmission line becomes reciprocal. The agreement of our results to those published in [24] (for both magnetization directions) is very good keeping in mind that a cylindrical structure is considered here as compared to a planar one in [24]. This shows again the validity and versatility of the developed FDTD and SDA algorithms. It should be mentioned that the same FDTD code that was used to analyze the cylindrical microstrip line is used here. One has only to specify the dielectric and ferrite layers and their thicknesses, besides specifying the metallization.

IV. CONCLUSIONS

Efficient 2-D FDTD and spectral-domain algorithms in cylindrical coordinates, which are suitable to analyze cylindrical transmission lines printed on magnetized ferrite, have been developed. Several representative cylindrical structures have been investigated and the results have been validated by comparing them to published numerical data. Specifically, the cylindrical microstrip line, and the CCPW have been studied.

REFERENCES

[1] O. Civi and A. Hizal, "Microstrip patch antenna on magnetized cylindrical ferrite substrate," in *IEEE AP-S Symp. Dig.*, Montreal, QC, Canada, July 1997, pp. 1516–1519.
[2] ——, "Effects of anisotropy of ferrite coating on the radiation characteristics of a cylindrical conductor excited by elementary sources," *J. Electromagn. Waves Applicat.*, vol. 12, pp. 287–307, 1998.
[3] H. Yang and P. Uslenghi, "Radiation characteristics of microstrip antennas on cylindrical bianisotropic substrates," *Electromagnetics*, vol. 15, pp. 499–511, 1995.
[4] K. Ivanov, "Propagation along azimuthally magnetized ferrite loaded circular guide," *Radio Sci.*, vol. 19, no. 5, pp. 1305–1310, Sept./Oct. 1984.
[5] K. Ivanov and R. Pregla, "Analysis of circular waveguides with azimuthally magnetized ferrite," in *Proc. 27th Eur. Microwave Conf.*, Sept. 1997, pp. 229–231.
[6] G. Chinn, L. Epp, and G. Wilkins, "Determination of the eigenfrequencies of a ferrite-filled cylindrical cavity resonator using the finite element method," *IEEE Trans. Microwave Theory Tech.*, vol. 43, pp. 1207–1209, May 1995.
[7] N. Dib and T. Weller, "Two dimensional finite difference time domain analysis of cylindrical transmission lines," *Int. J. Electron.*, vol. 87, no. 9, pp. 1065–1081, Sept. 2000.
[8] H. Yang, "Microstrip open-end discontinuity on a nonreciprocal ferrite substrate," *IEEE Trans. Microwave Theory Tech.*, vol. 42, pp. 2423–2428, Dec. 1994.
[9] I. Hsia, H. Yang, and N. Alexopoulos, "Basic properties of microstrip circuit elements on nonreciprocal substrate-superstrate structures," in *IEEE MTT-S Symp. Dig.*, 1990, pp. 665–668.
[10] N. Dib, T. Weller, M. Scardelletti, and M. Imparato, "Analysis of cylindrical transmission lines with the finite difference time domain method," *IIEEE Trans. Microwave Theory Tech.*, vol. 47, pp. 509–512, Apr. 1999.
[11] M. Okoniewski and E. Okoniewska, "FDTD analysis of magnetized ferrites: A more efficient algorithm," *IEEE Microwave Guided Wave Lett.*, vol. 4, pp. 169–171, June 1994.
[12] J. Lenge, A. Ahland, J. Kastner, and D. Schulz, "FDTD analysis of microwave circulators involving saturated magnetized ferrites," in *Int. IEEE MTT Symp. Dig.*, 1998, pp. 633–636.
[13] B. Yildrim and E. Al-Sharawy, "FDTD analysis of a stripline disc junction circulator," in *Int. IEEE MTT Symp. Dig.*, 1998, pp. 629–632.
[14] Y. Nishioka, O. Maeshima, T. Uno, and S. Adachi, "FDTD analysis of resistor-loaded bow-tie antennas covered with ferrite-coated conducting cavity for subsurface radar," *IEEE Trans. Antennas Propagat.*, vol. 47, pp. 970–977, June 1999.
[15] T. Monediere, K. Pichavant, F. Marty, P. Gelin, and F. Jecko, "FDTD treatment of partially magnetized ferrites with a new permeability tensor model," *IEEE Trans. Microwave Theory Tech.*, vol. 46, pp. 983–987, July 1998.
[16] G. Zheng and K. Chen, "Transient analysis of microstrip lines with ferrite substrate by extended FDTD method," *Int. J. Infrared Millim. Waves*, vol. 13, no. 8, pp. 1115–1125, 1992.
[17] A. Reineix, T. Monediere, and F. Jecko, "Ferrite analysis using the FDTD method," *Microwave Opt. Technol. Lett.*, vol. 5, no. 13, pp. 685–686, Dec. 1992.
[18] J. Pereda, L. Vielva, A. Vegas, and A. Prieto, "FDTD analysis of magnetized ferrites: An approach based on the rotated Richtmyer difference scheme," *IEEE Microwave Guided Wave Lett.*, vol. 3, pp. 322–324, Sept. 1993.
[19] J. Pereda, L. Vielva, A. Vegas, and A. Prieto, "A treatment of magnetized ferrites using the FDTD method," *IEEE Microwave Guided Wave Lett.*, vol. 3, pp. 136–138, May 1993.
[20] J. Pereda, L. Vielva, M. Solano, A. Vegas, and A. Prieto, "FDTD analysis of magnetized ferrites: Application to the calculation of dispersion characteristics of ferrite-loaded waveguides," *IEEE Trans. Microwave Theory Tech.*, vol. 43, pp. 350–357, Feb. 1995.
[21] J. Pereda, L. Vielva, A. Vegas, and A. Prieto, "An extended FDTD method for the treatment of partially magnetized ferrites," *IEEE Trans. Magn.*, vol. 31, pp. 1666–1669, May 1995.
[22] E. Yung, R. Chen, Y. Wang, and K. Wu, "FDTD analysis of EM wave circulated by a magnetized ferrite body of arbitrary shape," *Proc. IEE—Microwave Antennas Propagat.*, vol. 145, no. 6, pp. 433–440, Dec. 1998.

[23] M. Kales, "Modes in waveguides containing ferrites," *J. Appl. Phys.*, pp. 604–608, 1953.
[24] L. Zhou and L. Davis, "FEM analysis of coplanar waveguide with ferrite magnetized in an axial or transverse direction," *IEEE Trans. Magn.*, vol. 33, pp. 1410–1413, Mar. 1997.

Nihad Dib (S'89–M'92–SM'99) received the B.Sc. and M.Sc. degrees in electrical engineering from Kuwait University, Kuwait, in 1985 and 1987, respectively, and the Ph.D. degree in electrical engineering (major in electromagnetics and microwaves) in 1992 from the University of Michigan, Ann Arbor.

He was an Assistant Research Scientist in the Radiation Laboratory at the University of Michigan. In September 1995, he joined the Electrical Engineering Department, Jordan University of Science and Technology (JUST), Irbid, Jordan, as an Assistant Professor, and became an Associate Professor in September 2000. Since July 2001, he has been a Senior Research Engineer with Ansoft Corporation, Elmwood Park, NJ, on sabbatical leave from JUST. His research interests are mainly in computational electromagnetics. He is a member of the Editorial Board of *Electronics Letters*.

Dr. Dib is a member of the Editorial Board of the IEEE TRANSACTIONS ON MICROWAVE THEORY AND TECHNIQUES.

Amjad Omar was born in Kuwait in 1963. He received the B.Sc. and M.Sc. degrees in electrical engineering from Kuwait University, Kuwait, in 1985 and 1988, respectively, and the Ph.D. degree from the University of Waterloo, Waterloo, ON, Canada, in 1993.

From 1993 to 1994, he was a Visiting Post-Doctoral Fellow at the Communications Research Center, Ottawa, ON, Canada. From 1994 to 1996 he was an Assistant Professor at Amman University, Jordan. From 1996 to 1997, he was at the Royal Scientific Society, Jordan. From 1997 to 1999, he was at the United Arab Emirates University at Al-Ain. Since then, he has been with Hashemite University, Zarqa, Jordan, where he is currently Chairman of the Department of Electrical and Computer Engineering. He spent two months as a Research Associate at the Royal Military College, Canada, in 1999. He also spent three months as a Visiting Assistant Professor at the University of Waterloo in 2001. His research interests are in the numerical solution of microwave and millimeter-wave integrated circuits, dual-frequency antennas, microwave filter design, and analysis.